Contents lists available at ScienceDirect

Arabian Journal of Chemistry

journal homepage: www.ksu.edu.sa

Original article

Identification and quantitation of NF-κB inhibitory components in weichang'an pill based on UHPLC-QE-MS and spectrum-effect relationship

Xiaoxia Cao [a,b,1], Cunyu Hu [a,b,1], Fei Shang [a,b], Yingshuang Lv [a,b], Ziyan Bian [a,b], Qing Yuan [a,b], Han Zhang [a,b], Yi Wang [a,b], Nan Li [a,b], Lin Wang [c], Yujing Wang [c], Yingjie Sun [c], Lin Miao [a,b], Yanxu Chang [a,b], Yuefei Wang [a,b], Wenzhi Yang [a,b], Lijuan Chai [a,b,*], Peng Zhang [a,b,*]

[a] State Key Laboratory of Component-based Chinese Medicine, Tianjin Key Laboratory of TCM Chemistry and Analysis, Tianjin University of Traditional Chinese Medicine, Tianjin 301617, China
[b] Haihe Laboratory of Modern Chinese Medicine, Tianjin 301617, China
[c] Lerentang Pharmaceutical Factory, Tianjin Pharmaceutical Da Ren Tang Group Corporation Ltd, Tianjin 300112, China

ARTICLE INFO

Keywords:
Weichang'an pill
NF-κB inhibitory activity
Spectrum-effect relationship
Quality control of TCM

ABSTRACT

Weichang'an pill (WCAP) is a traditional Chinese patent medicine, which is clinically used for the treatment of bowel syndrome and functional dyspepsia such as diarrhea, abdominal distension, and enteritis. So far, quality control studies of WCAP have mainly focused on the determination of chemical composition content, which has little relevance to biological activity and clinical effects. With the aim of identifying the multi-index ingredients with NF-κB inhibitory activities related to WCAP clinical effect, this present work described the chemical profile of WCAP by UHPLC-QE-MS, established the correlated relationship between chromatographic fingerprints and the NF-κB inhibitory activities based on multivariate statistical analysis, including hierarchical clustering analysis (HCA), Pearson correlation analysis, and Partial least squares regression analysis (PLSR). The spectrum-effect relationship analysis indicated 10 compounds, which were ferulic acid, naringin, narirutin, hesperidin, neohesperidin, aloe emodin, emodin, honokiol, magnolol, and physcion, might be the potential NF-κB inhibitory constituents in the pill. The NF-κB inhibitory effects of the ten compounds were verified by *in vitro* dual luciferase reporting detection system. Considering that the detection index should be representative of more medicinal materials, a rapid and efficient UPLC-DAD method was eventually developed to determine the content of the 13 components. Our findings will provide data support for WCAP quality control and advance the understanding of the quality assessment of traditional Chinese patent medicines.

1. Introduction

WCAP, recorded in the first part of Chinese Pharmacopoeia in the 2020 edition (Commission, 2020), is composed of ten herbs, such as principal herbs *Santali Albi Lignum*, *Aucklandiae Radix,* and *Magnoliae Officinalis Cortex*. All the herbs are crushed to a fine powder, mixed together, and made into water pills. The protected medication has been widely used in China for more than 30 years to treat gastrointestinal diseases including enteritis, diarrhea, bacillary dysentery, stomach aches, abdominal pain, and abdominal distension (Shang et al., 2020; Shi et al., 2018). These diseases are often accompanied by inflammating, for example, enterities is an actue inflammation of ganstrointestinal mocosa, bacilary dysentery is a purulent inflammation of the colon caused by Shigella dysenteriae, manifested as abdominal pain, diarrhea, pus, and bloody stool and other clinical manifestations (Zhang et al., 2020). WCAP methanol extraction could significantly improve the 5-fluorouracil-induced intestinal mucositis mice, the inflammatory factors NF-κB, IL-1β were significant decrease in the IM mice (Chen et al., 2016).

The nuclear factor κB (NF-κB) is one of the most critical regulatory factors involved in inflammation which can induce the gene expression of cytokines and the transcription factors in the regulation of inflammatory responses (Kunnumakkara et al., 2020; Yu et al., 2020). The activation of NF-κB is the decisive factor of many pathological

Peer review under responsibility of King Saud University.
* Corresponding authors.
E-mail addresses: cljuan1258@163.com (L. Chai), zhangpeng@tjutcm.edu.cn (P. Zhang).
[1] Co-first authors: Xiaoxia Cao and Cunyu Hu contributed equally to this work and should be considered co-first authors

https://doi.org/10.1016/j.arabjc.2023.105328
Received 28 March 2023; Accepted 2 October 2023
Available online 18 October 2023

conditions, which makes it a therapeutic target for the clinical treatment of related diseases., NF-κB is a common index in gastrointestinal inflammation effect evaluation. A significant increase of NF-κB was observed in rats with gastritis (Xu et al., 2022), and a decrease of NF-κB p65 was also observed in DSS-induced chronic colitis mice after treatment with asperuloside (Chen et al., 2021). Therefore, compounds with NF-κB inhibition may serve as candidates for quality control indicators of WCAP. Single-component inhibitory activity of NF-κB, such as magnolol and honokiol, have been reported (Chen et al., 2019; Tse et al., 2005), but the overall picture of the NF-κB inhibitory component in WCAP remains unclear. WCAP and its components with NF-κB inhibitory activity were studied by using a TNF-α-induced dual luciferase reporting assay system in HEK 293 cells (Han et al., 2015).

Currently, 41 chemicals from the WACP methanol extract have been identified by HPLC-ESI-MS/MS (Liu et al., 2013). The identified compounds were from *Radix et Rhizoma Rhei*, *Fructus Aurantii*, *Cortex Magnoliae officinalis,* and *Radix Aucklandiae*, while the chemical compositions of the other six herbs remained unknown. Quality control studies at WCAP have determined the chemical composition content of 14 compounds from five herbs (Zhang et al., 2010; Jing et al., 2012; Zhang et al., 2013). However, there is a lack of systematic studies on the biological activity of WCAP quality control indicators. The composition of WCAP is too complex, and some of the components are difficult to obtain, making it difficult to detect their activities one by one. Spectrum-effect relationship investigations have been proposed as a potential method to predict effective components in complex mixtures and to mirror the internal quality of herbal medicines (Zhu et al., 2016). PLSR and artificial neural network were used to explore the spectrum-effect relationship of *Sinomenii Caulis*, and 8 potential anti-inflammatory components were screened out from a total of twenty two components (Wang et al., 2019). Other statistical methods such as Pearson correlation analysis have also been widely used to investigate the spectrum-effect relationship (An et al., 2022).

This present work described the identification and quantitation of NF-κB inhibitory components in WCAP based on UHPLC-QE-MS and spectrum-effect relationship. The chemical profile of WCAP was investigated by UHPLC-QE-MS, and 129 chemical constituents were identified from eight herbs. UPLC-UV fingerprints of 16 batches of WCAP were established, and their NF-κB inhibitory activities were detected by the TNF-α-induced dual luciferase reporting assay system in HEK 293 cells. The spectrum-effect relationship indicated 10 compounds, as well as ferulic acid, naringin, narirutin, hesperidin, neohesperidin, aloe emodin, emodin, honokiol, magnolol, physcion, might be potential NF-κB inhibitory constituents and their effects were verified. To cover more medicinal material quality control, a rapid and efficient UPLC-DAD method was subsequently developed to determine the content of the 10 components plus rhein, costunolide and chrysophanol. The result will provide data support for WCAP quality control improvement.

2. Material and methods

2.1. Materials and reagents

Sixteen batches of WCAP were produced by Tianjin Zhongxin Pharmaceutical Group Corporat Lerentang Pharmaceutical Factory, the details of which are given in Table S1. Methanol, acetonitrile and formic acid were purchased from Fisher Scientific and Tianjin Obt Chemical Co., LTD, ferulic acid, narirutin, naringin, hesperidin, neohesperidin, aloe emodin, rhein, emodin, honokiol, costunolide, dehydrocostus lactone, magnolol, chrysophanol, and physcion were obtained from Sichuan Weikeqi Technology Co., Ltd. TNF-α, human embryonic kidney cell 293 (HEK293), NF-κB luciferase reporter plasmid PGL 4.32 and sea kidney luciferase reporter plasmid PRL-TK was purchased from PeproTech.

2.2. Sample extraction

50 mg WCAP powder was immersed in 500 μL 80 % methanol, swirled for 30 s, ultrasonic extraction for 1 h, and centrifuged at 12000 rpm for 15 min. The supernatant was filtered by 0.22 μm microporous filter membrane and then sampled to inject for LC-MS analysis.

An aliquot of 1.0 g of sixteen batches of WCAP powder was immersed in 20 mL methanol, followed ultrasonic extraction at room temperature for 90 min, the mixture was then centrifuged at 13,000 rpm for 10 min. The supernatant was filtered through a 0.45 μm nylon syringe filter and stored at before the UPLC analysis.

2.3. UHPLC-QE-MS analysis

LC-MS/MS analysis was performed on an Agilent ultra-high performance liquid chromatography 1290 UPLC system with a Waters UPLC BEH C_{18} column (2.1 mm × 100 mm, 1.7 μm). The column temperature was set at 55 ℃ and the sample injection volume was set at 5 μL. The flow rate was set at 0.5 mL/min. The mobile phase consisted of 0.1 % formic acid in water (A) and 0.1 % formic acid in acetonitrile (B). The multi-step linear elution gradient program was as follows: 0 – 11 min, 15 – 75 % B; 11 – 12 min, 75 – 98 % B; 12 – 14 min, 98 – 98 % B; 14 – 14.1 min, 98 – 15 % B; 14.1 – 16 min, 15 – 15 % B.

A Q Exactive Focus mass spectrometer coupled with Xcalibur software was employed to obtain the MS and MS/MS data based on the IDA acquisition mode. During each acquisition cycle, the mass range was from 100 to 1500, and the top three of every cycle were screened and the corresponding MS/MS data were further acquired. Sheath gas flow rate: 45 Arb, Aux gas flow rate: 15 Arb, Capillary temperature: 400 ℃, Full ms resolution: 70000, MS/MS resolution: 17500, Collision energy: 15/30/45 in NCE mode, Spray Voltage: 4.0 kV (positive) or −3.6 kV (negative).

2.4. UPLC fingerprints

2.4.1. UPLC condition

The prepared samples were injected into a Waters ACQUITY UPLC system (Waters, Milford, MA, USA) with a photodiodearray (PDA) detector. The chromatographic separation was performed with a Waters ACQUITY UPLC BEH C_{18} column (2.1 mm × 100 mm, 1.7 μm), operated at 35°C. The flow rate was kept constant at 0.3 mL/min and UV measurements were obtained at 254 nm. The mobile phases were water contain 0.1 % Formic acid (A) and acetonitrile (B) with gradient elution was the following program: 0 – 3 min, 5 – 22.5 % B, 3 – 7 min, 22.5 – 22.5 % B, 7 – 8 min, 22.5 – 47 % B, 8 – 13 min, 47 – 47 % B, 13 – 14 min, 47 – 65 % B, 14 – 19 min, 65 – 65 % B, 19 – 20 min, 65 – 95 % B.

2.4.2. Method validation

The precision was certificated by evaluating six injections of the same working solution, repeatability was determined by the relative standard deviation (RSD) from six working solutions of the same sample, and the stability was analyzed by the same sample using the above-established method at 0, 2, 4, 8, 16, 24 h. The RSDs of precision were calculated based on the relative peak area of each characteristic peak, and the RSDs of repeatability and stability were calculated by mass concentration. Sample 1,530,963 was selected as sample solution for method validation and 13 main peaks were chosen for calculating the RSDs. Accuracy was determined by the recovery test. The mixed standard solutions were added to known amounts of samples, and then the resultant samples were extracted and analyzed by the established UHPLC method. The percentage recoveries were evaluated by calculating the ratio of the detected amount versus added amount.

2.4.3. Establishment and evaluation of fingerprints

To determine a representative chromatographic fingerprints, 16 batches of WCAP were analyzed with the optimal UPLC method. Chemometrics were applied to demonstrate the differences in the 16 batches

of WCAP. Similarity analysis was performed by the Similarity Evaluation System for Chromatographic Fingerprints of Traditional Chinese Medicines (version 2012A; Beijing, China). Hierarchical cluster analysis (HCA) of the 16 samples was performed using SIMCA14.1.

2.5. NF-κB inhibitory activity assay

293 T cells were plated 3 × 10^4/well in 96 well in DMEM supplemented with 10 % FBS, 100 U/mL penicillin, and 100 μL streptomycin at 37.5 °C in a humidified atmosphere containing 5 % CO_2.. When the cell reaches about 80 % confluency, the NF-κB luciferase reporter plasmid pGL4.32 (100 ng/well) and the sea chenin luciferase reporter plasmid pRL-TK (9.6 ng/ well) were transfected into cells with PEI (1 mg/mL) transfection reagent and cultured for 24 h (Makó et al., 2010; Gordon et al., 2011). After 24 h culture, TNF-α (10 ng/mL) was added into each well as the model group, Dex (0.01 μM, Dexamethason) + TNF-α (10 ng/mL) as the positive drug group, and each batch of WCAP to be tested (0.001 μg/mL) + TNF-α (10 ng/mL) as the experimental group, a blank control was set and cultured for 6 h. After 6 h incubation at 37.5 °C, cells were washed with PBS and detected by dual luciferase detection system after lysis. The ratio of firefly luciferase activity to sea kidney luciferase activity was calculated to obtain the relative luciferase activity value (Gordon et al., 2011), Each group was set up with six duplicate holes and repeated three times. The NF-κB inhibition activity of 16 batches of methanol extracts from WCAP was determined by Multilabel Plate Reader (Perkins Elmer).

2.6. Spectrum-effect relationship

2.6.1. Pearson correlation analysis

Correlation analysis is a statistical analysis method to study the correlation between two or more random variables. Pearson correlation coefficient is a coefficient to measure the linear relationship between distance variables (Han et al., 2021). The index components of NF-κB inhibitory activity were analyzed by the Pearson correlation coefficient.

2.6.2. Partial least squares regression analysis (PLSR)

PLSR is a multivariate analysis method, which is a linear regression model to find and explain the relationship between a dependent variable and an independent variable. It combines multiple linear regression, canonical correlation analysis, and principal component analysis to overcome multicollinearity caused by multiple independent variables (Chen et al., 2020), and is more comprehensive and comprehensive than the above correlation analysis. In this experiment, PLSR was analyzed using SIMCA14.1.

2.6.3. Statistical analysis

SPSS17.0 was used for statistical analysis, and the results were expressed as mean standard deviation ($\bar{x} \pm SD$). Univariate analysis of variance was used between groups, and the difference was statistically significant when $p < 0.05$.

3. Results and discussion

3.1. UHPLC-QE-MS profiling of WCAP

A total of 129 compounds were identified from *Fructus Aurantii*, *Cortex Magnoliae officinalis*, *Radix et Rhizoma Rhei*, *Radix Aucklandiae*, *Aquilariae Lignum Resinatum*, *Jujubae Fructus*, *Chuanxiong Rhizoma,* and *Crotonis Semen Pulveratum* respectively. It mainly includes flavonoids, phenylpropanoids, alkaloids, etc. The total ion flow diagram of UHPLC-QE-MS is shown in Fig. 1, and the identification results of UHPLC-QE-MS are shown in Table 1 and Table 2.

3.2. UPLC fingerprints analyze

3.2.1. Method validation for UPLC fingerprints

The results of the method validation showed that the RSDs of

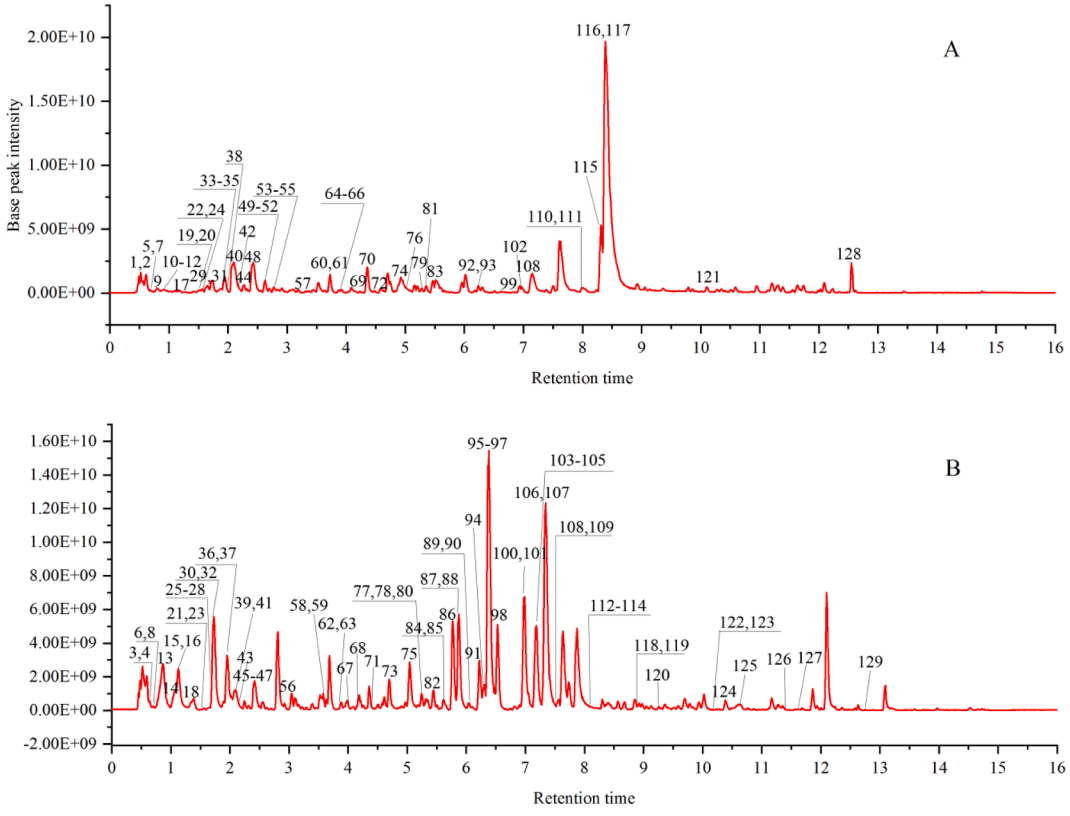

Fig. 1. Total ion chromatograms of WCAP by UHPLC-QE-MS, under negative (A) and positive (B) ionization modes.

Table 1
Information on 129 compounds in WCAP methanol extracts identified by UHPLC-QE-MS.

No.	t_R(min)	Experimental (*m/z*)	Ion mode	Error (ppm)	MS/MS	Molecular formula	Identification	Distribution
1	0.59	134.0473	[M−H]-	2.41	119.0350	C5H5N5	Adenine	JF
2*	0.62	169.0141	[M−H]-	0.50	125.0249	C7H6O5	Gallic acid	RRR
3	0.63	168.1020	[M + H]±	−2.83	150.0913;135.0677;119.0897;107.4177	C9H13NO2	Synephrine	FA
4	0.64	152.1071	[M + H]±	−2.89	121.0648	C9H13NO	N-Methyltyramine	FA
5	0.68	483.0781	[M−H]-	1.29	465.1033;439.0866;321.0825;169.0141;151.0398;125.0245	C20H20O14	Gallic acid-*O*-galloyl-glucoside	RRR
6	0.72	330.1704	[M + H]±	1.24	299.1242;192.1042;177.0547;137.0597	C19H23NO4	Sinomenine	CMO
7*	0.75	153.0191	[M−H]-	0.89	109.0293	C7H6O4	Protocatechuic acid	CR
8	0.75	265.1551	[M + H]±	−0.55	177.0547;145.0496	C14H20N2O3	N-Feruloylputrescine	CMO
9	0.79	785.2503	[M−H]-	−0.13	477.1615;161.0456	C35H46O20	Magnoloside B	CMO
10	0.83	289.0715	[M−H]-	1.79	245.0667;203.0675;137.0245;109.0293	C15H14O6	Cianidanol	RRR
11	0.94	635.0893	[M−H]-	1.37	465.1414;169.0141	C27H24O18	Gallic acid-*O*-digalloyl-glucoside	RRR
12*	0.94	167.0348	[M−H]-	2.39	152.0354;123.0086;108.0455	C8H8O4	Vanillic acid	FA
13	0.98	313.1591	[M + H]±	−3.03	205.1099;190.0863	C19H22NO3 ±	3,4-Dehydromagnocurarine	CMO
14	1.05	166.1227	[M + H]±	1.72	151.0393;137.0597	C10H15NO	Hordenine	FA
15	1.11	344.1853	[M + H]±	−2.56	299.1473;175.1118;151.0393;137.0597	C20H26NO4 ±	Tembetarine	CMO
16*	1.12	342.1699	[M + H]±	−0.29	297.1118;265.1437	C20H24NO4 ±	Magnoflorine	CMO
17	1.13	507.1138	[M−H]-	−0.24	345.1557;331.1756;313.0576;169.0141;151.0400;125.0242	C23H24O13	Ferulic acid-*O*-galloyl-glucoside	RRR
18	1.42	611.1605	[M + H]±	0.90	465.1035;303.0497;153.0548	C27H30O16	Rutin	FA
19	1.43	325.0932	[M−H]-	0.57	235.0609;163.0399;145.0297;119.0503	C15H18O8	*p*-Coumaric acid-*O*-glucoside	RRR
20	1.45	623.1991	[M−H]-	1.78	461.2038;315.1082;161.0456;135.0452	C29H36O15	Magnoloside A	CMO
21	1.50	417.1184	[M + H]±	1.04	375.1444;336.1804;255.1743;185.1329	C21H20O9	Daidzin	RRR
22	1.55	729.1461	[M−H]-	0.66	577.1562;381.1353	C37H30O16	Proanthocyanidins B-*O*-gallate	RRR
23	1.55	451.1230	[M + H]±	−2.20	397.1488;163.0394;289.0703	C21H22O11	Eriodictyol-7-*O*-Glucoside	FA
24	1.56	441.0823	[M−H]-	0.77	331.1395;289.0749;245.1031;205.0508;203.9948;193.0502;179.0562;169.0141;125.0242	C22H18O10	Epicatechin gallate	RRR
25	1.57	373.1488	[M + H]±	−2.93	211.1321;193.0860	C17H24O9	Syringin	CMO
26	1.67	183.0653	[M + H]±	1.40	155.0702;140.0468;125.0597	C9H10O4	Syringaldehyde	AR
27	1.67	595.1663	[M + H]±	0.56	449.1079;287.0547	C27H30O15	Lonicerin	FA
28*	1.71	195.0655	[M + H]±	2.31	177.0457;149.0598;134.0802;117.0701	C10H10O4	Ferulic acid	FA/CR
29	1.71	541.1362	[M−H]-	2.99	313.1298;227.1293;169.0141;125.0242	C27H26O12	Resveratrol-*O*-galloyl-glucoside	RRR
30*	1.72	319.1179	[M + H]±	0.43	301.1066;283.0989;255.1020;227.1061;164.0979	C17H18O6	Agarotetrol	ALR

(*continued on next page*)

Table 1 (*continued*)

No.	t_R(min)	Experimental (*m/z*)	Ion mode	Error (ppm)	MS/MS	Molecular formula	Identification	Distribution
31	1.74	477.1046	[M−H]-	2.71	331.0825;315.1240;313.0562;169.0141;151.0398;125.0242	C22H22O12	*p*-Coumaric acid-*O*-galloyl-glucoside	RRR
32	1.79	268.1335	[M + H]±	−1.09	251.1082;219.0287;191.1068	C17H17NO2	Asimilobine	CMO
33	1.87	547.1461	[M−H]-	1.61	233.0450;191.0555;177.0924;169.0141;151.0396;125.0243	C26H28O13	2-(2′-Hydroxypropyl)-5-methyl-7-hydroxychromone-*O*-galloyl-glucoside	RRR
34*	1.89	861.1887	[M−H]-	1.00	721.1888;465.1038	C42H38O20	Sennoside B	RRR
35	1.91	515.1186	[M−H]-	0.74	353.0879;191.0555;173.0607	C25H24O12	Isochlorogenic acid A	AR
36	1.92	314.1747	[M + H]±	−3.02	269.1363;237.1849;175.1118;107.0856	C19H24NO3 ±	Magnocurarine	CMO
37	1.95	319.1175	[M + H]±	−2.27	301.1076;283.0966;255.1019;227.1089;164.0704	C17H18O6	Aquilarone B	ALR
38	1.98	603.1304	[M−H]-	−7.55	451.1042;289.0714;245.1022;227.0344;205.0348;179.0562;161.0451;137.0242	C28H28O15	Catechin-*O*-galloyl-glucoside/ Epigallocatechin-*O*-gallate glucoside	RRR
39	2.08	579.1703	[M + H]±	1.16	433.1122;271.0595;253.1797;235.0968	C27H30O14	Rhoifolin	FA
40*	2.08	579.1730	[M−H]-	2.76	271.0616;151.0394;119.0500	C27H32O14	Narirutin	FA
41	2.09	435.1282	[M + H]±	0.47	273.0762;231.1379;195.0289;153.0181	C21H22O10	Naringenin-7-*O*-glucoside	FA
42	2.18	515.1187	[M−H]-	0.60	353.0878;191.0195;179.0558;173.0448	C25H24O12	Isochlorogenic acid B	AR
43	2.19	181.0497	[M + H]±	1.87	163.0389;145.0496;137.0963	C9H8O4	Caffeic acid	FA
44	2.28	881.1575	[M−H]-	1.09	577.2874;559.2029;541.1334;533.1322;493.1146;467.1194;449.1094;407.1347;381.0740;289.0713;245.0813	C44H34O20	Proanthocyanidins B-*O*-digallate	RRR
45	2.30	597.1820	[M + H]±	0.09	289.0705;163.1120	C27H32O15	Eriocitrin	FA
46	2.42	465.1390	[M + H]±	−1.40	303.0875;153.0173;151.0754	C22H24O11	Hesperetin 7-*O*-glucoside	FA
47	2.42	595.2011	[M + H]±	−2.74	449.1437;287.1276;272.1275;254.1826	C28H34O14	Didymin	FA
48*	2.43	609.1823	[M−H]-	0.46	301.0699	C28H34O15	Hesperidin	FA
49	2.52	613.1184	[M−H]-	−1.49	569.2242;443.1700;169.0141;147.0448;125.0242	C29H26O15	Cinnamoyl-*O*-digalloyl-glucoside	RRR
50*	2.56	579.1731	[M−H]-	1.88	459.0927;271.0611;151.0396	C27H32O14	Naringin	FA
51	2.62	493.1148	[M−H]-	−9.09	331.1393;313.0560;169.0131;151.0028;125.0240	C19H26O15	Gallic acid-*O*-diglucoside	RRR
52	2.65	461.1082	[M−H]-	1.63	401.0567;313.0561;211.0972;193.0501;169.0139;151.0398	C22H22O11	1-*O*-Galloyl-6-*O*-cinnamoyl-glucose	RRR
53	2.80	445.0774	[M−H]-	0.79	325.1294;297.0758;283.1548;269.0450;263.1285;239.1292;235.0612;211.0971;207.0656	C21H18O11	Rhein 8-*O*-glucoside	RRR
54	2.94	861.1890	[M−H]-	1.34	465.2699	C42H38O20	Sennoside A	RRR
55*	2.97	609.1823	[M−H]-	0.66	301.0706;286.0467	C28H34O15	Neohesperidin	FA
56	3.03	203.0342	[M + H]±	0.89	131.0495;119.0857	C11H6O4	Xanthotoxol	FA
57	3.43	407.1348	[M−H]-	0.60	245.1387;215.0326	C20H24O9	Torachrysone 8-O-glucosid	RRR
58	3.59	271.0967	[M + H]±	2.60	203.1428;159.1167;147.0442;131.0491	C16H14O4	Isoimperatorin	FA
59	3.65	303.0860	[M + H]±	0.12	177.0538;153.0190	C16H14O6	Homoeriodictyol	FA
60*	3.74	271.0612	[M−H]-	0.69	187.0974;151.0031;119.0497	C15H12O5	Naringenin	FA
61	3.74	671.1798	[M−H]-	4.94	509.1069;389.1817;361.0929;227.1293;183.1027;169.0141;151.0396;125.0245	C36H32O13	Resveratrol-*O*-cinnamoyl-galloyl-glucoside	RRR

(*continued on next page*)

Table 1 (*continued*)

No.	t_R(min)	Experimental (*m/z*)	Ion mode	Error (ppm)	MS/MS	Molecular formula	Identification	Distribution
62	3.76	315.0863	[M + H]±	1.07	300.1954;285.0757;272.0634;257.1897	C17H14O6	Baicalin 4′,7-dimethyl ether	FA
63	3.87	331.1170	[M + H]±	−3.50	313.1067;149.0598	C18H18O6	3-hydroxy-4′,5,7-trimethoxyflavanone	FA
64	3.89	517.0978	[M−H]-	−0.72	473.1078;269.0450;225.1128	C24H22O13	Emodin 8-*O*-6′′-malonylglucoside	RRR
65	3.92	299.1284	[M−H]-	0.32	239.1080	C18H20O4	Magnolignan A or C	CMO
66	3.96	623.1772	[M−H]-	1.12	459.1309;313.0351;307.1193;295.0972;169.0141;163.0400;151.0398;125.0245	C32H32O13	4-(4′-Hydroxyphenyl)-2-butanone-*O*-cinnamoyl-galloyl-glucoside	RRR
67	4.03	319.1542	[M + H]±	0.56	301.1451;177.0548;162.0914	C18H22O5	Pranferin	FA
68	4.16	237.1850	[M + H]±	−2.11	219.1734;201.1645	C15H24O2	Curcumol	ALR
69	4.32	431.0986	[M−H]-	1.43	269.0452;241.0874;240.0785;225.0921	C21H20O10	Emodin 8-O-glucoside	RRR
70	4.37	241.0866	[M−H]-	0.61	223.0761;197.0970;133.0139	C15H14O3	Randaiol	CMO
71	4.42	249.1486	[M + H]±	1.60	231.1379;203.1798;213.1277;185.1329;157.1015;143.0858	C15H20O3	Santamarine	AR
72	4.60	299.1283	[M−H]-	0.09	239.1073	C18H20O4	Magnolignan A or C	CMO
73	4.72	373.1281	[M + H]±	0.26	358.2371;343.0797;328.1017;315.1583;181.1211	C20H20O7	Isosinensetin	FA
74	4.95	297.0407	[M−H]-	2.53	253.0493;225.0540;210.0332	C16H10O6	6-Methylrhein	RRR
75	5.04	261.1119	[M + H]±	0.50	177.0.0547;149.0960;133.1012	C15H16O4	Meranzin	FA
76	5.08	501.1776	[M−H]-	2.91	337.1448;277.1077;193.0509	C26H30O10	4-(4′-Hydroxyphenyl)-2-butanone-*O*-feruloyl-glucoside	RRR
77	5.23	267.1017	[M + H]±	1.27	176.0917;161.1326;137.0597	C17H14O3	7-Hydroxy-2-(2-phenylethyl)chromone	ALR
78	5.27	471.2013	[M + H]±	0.63	425.1949;161.1326	C26H30O8	Limonin	FA
79*	5.28	269.0455	[M−H]-	1.86	240.0434;225.0573	C15H10O5	Aloe emodin	RRR
80	5.31	327.1228	[M + H]±	−1.27	221.1898;107.0854	C19H18O5	Qinanone G	ALR
81	5.36	633.1622	[M−H]-	2.27	461.1833;443.1268;313.0718;295.0611;151.0402;125.242	C33H30O13	2,5-Dimethyl-7-hydroxychromone-*O*-cinnamoyl-galloyl-glucoside	RRR
82	5.43	283.0968	[M + H]±	0.69	192.1099;164.1512	C17H14O4	6,8-Dihydroxy-2-(2-phenylethyl)chromone	ALR
83*	5.53	283.0247	[M−H]-	1.11	257.0459;239.0354	C15H8O6	Rhein	RRR
84	5.60	533.2388	[M + H]±	0.11	369.2067;161.1325	C28H36O10	Nomaline acid	FA
85	5.60	491.2279	[M + H]±	−0.37	449.1595;407.1484;347.1629;329.1216	C26H34O9	Sudachinoid A	FA
86	5.69	473.2167	[M + H]±	−1.79	427.1033;161.1326	C26H32O8	Deacetyl nomilin	FA
87	5.82	343.1172	[M + H]±	0.70	313.1069;285.0761	C19H18O6	6-Demethoxytangeretin	FA
88*	5.87	403.1383	[M + H]±	0.82	388.1144;373.0877;355.0781	C21H22O8	Nobiletin	FA
89	6.09	127.0391	[M + H]±	−3.28	109.1012	C6H6O3	5-Hydroxymethylfurfural	AR

(*continued on next page*)

Table 1 (*continued*)

No.	t_R(min)	Experimental (*m/z*)	Ion mode	Error (ppm)	MS/MS	Molecular formula	Identification	Distribution
90	6.12	311.1272	[M + H]±	−3.51	203.1797;190.1674;151.1118;121.1011	C19H18O4	6-Methoxy-2-[2-(3′-methoxyphenyl) ethyl] chromone	ALR
91	6.22	341.1380	[M + H]±	0.09	121.0638	C20H20O5	6,7-Dimethoxy-2-[2-(4′-methoxyphenyl) ethyl] chromone	ALR
92	6.25	355.1182	[M−H]-	2.23	311.2230;296.1008;281.0818	C20H20O6	Coniferyl ferulate	CR
93	6.29	171.1390	[M−H]-	0.09		C10H20O2	Decanoic acid	CSP
94*	6.31	193.1222	[M + H]±	1.08	175.1118;147.1168;137.0597;119.0852;105.0701	C12H16O2	Senkyunolide A	CR
95*	6.34	191.1067	[M + H]±	1.39	173.0963;145.1013	C12H14O2	3-*n*-Butylphathlide	CR
96	6.38	311.1272	[M + H]±	−3.38	220.0725;205.0489;181.0482	C19H18O4	6,7-Dimethoxy-2-(2-phenylethyl) chromone	ALR
97	6.48	419.1335	[M + H]±	−1.63	389.1964;371.1858;361.0899	C 21H 22O 9	Natsudaidain	FA
98*	6.53	373.1281	[M + H]±	0.23	343.0787;325.1429	C20H20O7	Tangeretin	FA
99	6.76	253.0871	[M−H]-	2.53	235.1339;207.0509	C16H14O3	Magnaldehyde D	CMO
100	6.94	389.1234	[M + H]±	1.12	374.1316;359.1842;341.1366	C20H20O8	5-*O*-Demethylnobiletin	FA
101	6.98	251.1063	[M + H]±	−3.72	173.0964;160.0511;121.0276	C17H14O2	2-(2-phenylethyl) chromone	ALR
102	7.02	329.1396	[M−H]-	2.27	267.1024;249.1491;239.0714;133.0142	C19H22O5	Magnolignan D	CMO
103	7.08	269.0452	[M−H]-	0.74	241.0875;225.0611;197.0618	C15H10O5	Emodin	RRR
104	7.10	379.1909	[M + H]±	0.05	361.1647;189.0913	C24H26O4	4,5-Dehydrodigestolide	CR
105	7.13	277.1802	[M + H]±	0.71	235.1693;199.0866;177.1273	C17H24O3	Ligustrosone	CR
106	7.33	281.1172	[M + H]±	−2.10	190.0615;151.0383	C18H16O3	6-Methoxy-2-(2-phenylethyl)chromone	ALR
107	7.42	189.0908	[M + H]±	1.14	147.1168;143.0858;133.1011	C12H12O2	3-Butylidenephthalide	CR
108	7.59	191.1067	[M + H]±	1.33	173.0954;145.1013	C12H14O2	Ligustilide	CR
109*	7.62	233.1534	[M + H]±	1.88	215.1427;187.1482;159.1168;145.1013;131.0857	C15H20O2	Costunolide	AR
110	7.82	297.1135	[M−H]-	2.58	249.1492;238.0898;231.9314	C18H18O4	Magnolignan E	CMO
111*	7.98	265.1232	[M−H]-	0.77	249.1488;224.0232;223.0759;209.0457;197.8081	C18H18O2	Honokiol	CMO
112*	8.17	231.1379	[M + H]±	0.30	213.1279;195.1181;185.1317;157.0645;143.0853	C15H18O2	Dehydrocostus lactone	AR
113	8.20	219.1747	[M + H]±	−0.91	201.1636;163.0753	C15H22O	Cyperotundone	ALR
114	8.27	207.1015	[M + H]±	2.20	165.0703;137.0600	C12H14O3	Acetyleugenol	AR
115	8.35	281.1177	[M−H]-	−0.51	263.1071;245.0958;133.0648	C18H18O3	Obovatol	CMO
116	8.56	295.1334	[M−H]-	−0.11	264.1148	C19H20O3	3-OMe-magnolol	CMO
117*	8.74	265.1232	[M−H]-	0.80	247.1129;245.0951;223.0788	C18H18O2	Magnolol	CMO
118	8.93	118.0862	[M + H]±	1.31	59.0483	C5H11NO2	Betaine	CMO
119	8.97	381.2055	[M + H]±	−2.91	335.2002;191.1067;173.0963	C24H28O4	Tokinolide B	CR
120	9.29	235.1693	[M + H]±	1.36	161.1326	C15H22O2	Costic acid	AR

(*continued on next page*)

Table 1 (*continued*)

No.	t_R(min)	Experimental (*m/z*)	Ion mode	Error (ppm)	MS/MS	Molecular formula	Identification	Distribution
121	10.23	279.1023	[M−H]-	0.84	261.0921;233.1547	C18H16O3	Randainal	CMO
122*	10.27	381.2055	[M + H]±	1.24	191.1069;173.0949;145.1015;105.0701	C24H28O4	Levistilide A	CR
123	10.31	299.1645	[M + H]±	1.70	175.1118;163.0389;119.0854;107.0854	C19H22O3	Auraptene	FA
124	10.45	179.1067	[M + H]±	−2.67	164.0425;151.0753;116.0703;123.0438	C11H14O2	Auraptene	AR
125	10.76	189.0546	[M + H]±	−3.28	131.0491;103.0541	C11H8O3	4′,5-Dihydropsoralen	FA
126	11.45	413.2330	[M + H]±	0.50	413.2330;223.1882;191.1068	C25H32O5	Wallichilide	CR
127	11.64	163.0389	[M + H]±	0.58	119.0334;107.0487	C9H6O3	7-Hydroxycoumarin	FA/CR
128	12.56	401.2490	[M−H]-	2.24	331.1696	C28H34O2	Piperitylmagnolol	CMO
129	12.75	415.3930	[M + H]±	−7.24	397.3102;367.3212;255.1741;213.1018	C29H50O	*β*-Sitosterol	FA/CR

note:*Represents comparison with the standards *Cortex Magnoliae officinalis*: CMO *Fructus Aurantii*: FA *Aquilariae Lignum Resinatum*: ALR *Radix et Rhizoma Rhei*: RRR *Aucklandiae Radix*: AR *Jujubae Fructus*: JF *Chuanxiong Rhizoma*: CR *Crotonis Semen Pulveratum*: CSP.

Table 2
Fingerprints similarity of chemical components in WCAP.

NO.	Similarity	NO.	Similarity
S605	0.856	S944	0.980
S826	0.996	S953	0.999
S932	0.996	S954	0.996
S936	0.994	S955	0.936
S938	0.995	S956	0.930
S939	0.996	S963	0.996
S940	0.999	S964	0.996
S942	0.999	S969	0.997

precision and repeatability were below 3.00 %. This means that the UPLC instrument was suitable for fingerprint analysis due to the good precision and repeatability of the UPLC fingerprint method. The RSD values of the major chromatograph peak area at different times were all less than 3.00 %, which indicates that the sample solution was stable within 24 h. The sample recovery rate ranges from 98.83 % to 103.15 %, The RSDs values of precision, reproducibility, stability, and recovery rate are shown in the supporting material (Table S2, S3, S4, S5).

3.2.2. UPLC fingerprints of WCAP samples and identification of common compounds

Import 16 batches of UPLC chromatograms of the main components of WCAP into the Similarity Evaluation System for Chromatographic Fingerprints of Traditional Chinese Medicines, use S1 as the reference spectrum, set a time window of 0.1, and use the median method to generate the control spectrum for fingerprint matching, the chromatographic fingerprints of the 16 batches were shown in Fig. 2A. 14 common peaks were obtained by retention time and reference substance. The UPLC chromatogram of reference substance was present in Fig. 2B, 14 common peaks (1 – 14) were identified as ferulic acid, narirutin, naringin, hesperidin, neohesperidin, aloe emodin, rhein, emodin, honokiol, costunolide, dehydrocostus lactone, magnolol, chrysophanol and physcion, respectively. The similarity calculation results show in Table 3 that the similarity of each batch of samples is greater than 0.90 (except S605). The relative peak areas and relative retention times of common peaks are presented in Table S6 and Table S7.

3.3. Hierarchical cluster analysis (HCA)

HCA was used to distinguish WCAP from different years by generating different clusters according to the similarity of fingerprints, and the result of HCA was shown in Fig. 3A. The result indicated that the samples were divided into two groups, S605 in group 1 and the rest of sample in group 2. The sum of the common peak areas of the 16 batches was made into a bar plot, which is shown in Fig. 3B. It can be seen from the bar chart and HCA results that the classification is related to the sum of the contents of the compounds.

3.4. NF-κB inhibitory activity test

NF-κB inhibitory activity was determined from the above 16 batches of WCAP methanol extract using the method of "2.5″. As shown in Table 3 and Fig. 4, the model group induced by TNF-α (10 ng/mL) significantly increased NF-κB activity. Compared with the Model group, each batch of samples significantly inhibited NF-κB inhibitory activity. Though S605 has the lowest sum of peak areas, its NF-κB inhibitory activity was not the weakest, which might be due to some strong activity coming from a low content compound.

3.5. Correlation analysis

The Pearson correlation analysis of NF-κB inhibitory activity and chemical components of the correlation analysis result is shown in Fig. 5A. The values range from −1 to 1. The larger the absolute value,

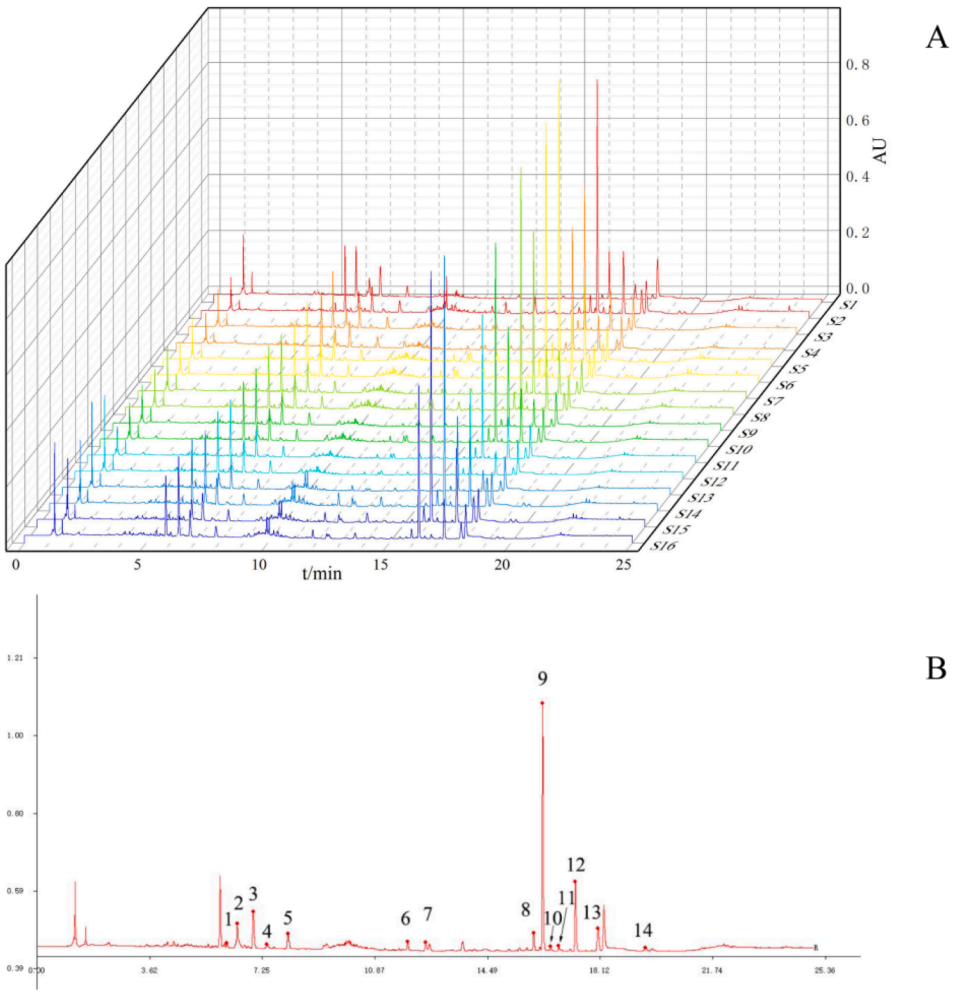

Fig. 2. UPLC fingerprints of 16 batches of WCAP methanol extracts (A), WCAP chemical components fingerprints control map1. Ferulic acid; 2. Narirutin; 3. Naringin; 4. Hesperidin; 5. Neohesperidin; 6. Aloe emodin; 7. Rhein; 8. Emodin; 9. Honokiol; 10. Costunolide; 11. Dehydrocostus lactone; 12. Magnolol; 13. Chrysophanol; 14. Physcion (B).

Table 3
NF-κB inhibitory activity of 16 batches WACP methanol extract.

number	NF-κB inhibitory activity	number	NF-κB inhibitory activity
S605	2476.99 ± 958.91	S944	3389.04 ± 852.86
S826	3383.59 ± 962.67	S953	4156.92 ± 464.89
S932	2408.56 ± 624.58	S954	2906.45 ± 837.65
S936	3385.08 ± 890.89	S955	4752.11 ± 860.41
S938	3415.84 ± 1022.92	S956	3039.59 ± 1082.51
S939	3499.08 ± 671.74	S963	4414.87 ± 667.42
S940	3735.95 ± 562.79	S964	3380.62 ± 556.82
S942	4393.00 ± 808.91	S969	3015.55 ± 409.27
Control	18.06 ± 2.80	Model	5717.10 ± 705.58
Dex	2504.64 ± 362.80		

the darker the color, and the smaller the absolute value, the weaker the correlation. An absolute value of 0.0 – 0.2 is a very weak correlation, 0.2 – 0.4 is a common correlation, 0.4 – 0.6 is a strong correlation. The Pearson correlation coefficients of each compound are shown in Table 4, The correlation analysis showed that the correlation coefficient with NF-κB inhibitory activity was classified narirutin (0.51), hesperidin (0.43), hesperidin (0.37), naringin (0.34), aloe emodin (0.34), ferulic acid (0.33), and honokiol (0.33), emodin (0.33), magnolol (0.32), and physcion (0.31). This analysis concluded that the flavonoid components, narirutin, naringin, hesperidin, and neohesperidin, made the greatest contribution to the inhibitory activity of NF-κB. Lignans and rhubarb anthraquinones are secondary, while the sesquiterpene components xylide and dehydroxylinol NF-κB contributed minor. The rhein correlation coefficient of −0.01 indicates that there is no obvious contribution to the inhibitory activity of NF-κB.

3.6. Partial least squares regression (PLSR) analysis

As shown in Fig. 5B, the Y regression equation for each explanatory variable is: $Y = 0.058X_1 + 0.196X_2 + 0.154X_3 + 0.138X_4 + 0.168X_5 + 0.055X_6\text{-}0.104X_7 + 0.044X_8 + 0.043X_9 + 0.019X_{10} + 0.035X_{11} + 0.036X_{12} + 0.015X_{13} + 0.035X_{14}$. The larger the regression coefficient, the more the compound contributed to the NF- κB inhibitory activity. The regression equation shows that the contribution of the compounds to NF-κB inhibitory activity was sorted as naringenin, neohesperidin, naringin, ferulic acid, aloe emodin, emodin, honokiol, magnolol, dehydrocostus lactone, physcion, chrysophanol, rhein.

Thus combining the Pearson correlation analysis and PLSR analysis, 10 compounds are likely to be active components to exert NF-κB inhibitory activity.

3.7. In vitro validation of active components

The NF-κB inhibitory activity was detected for the 10 chemical components. As shown in Fig. 6, except aloe emodin and physcion, the other 8 compounds showed significant activity.

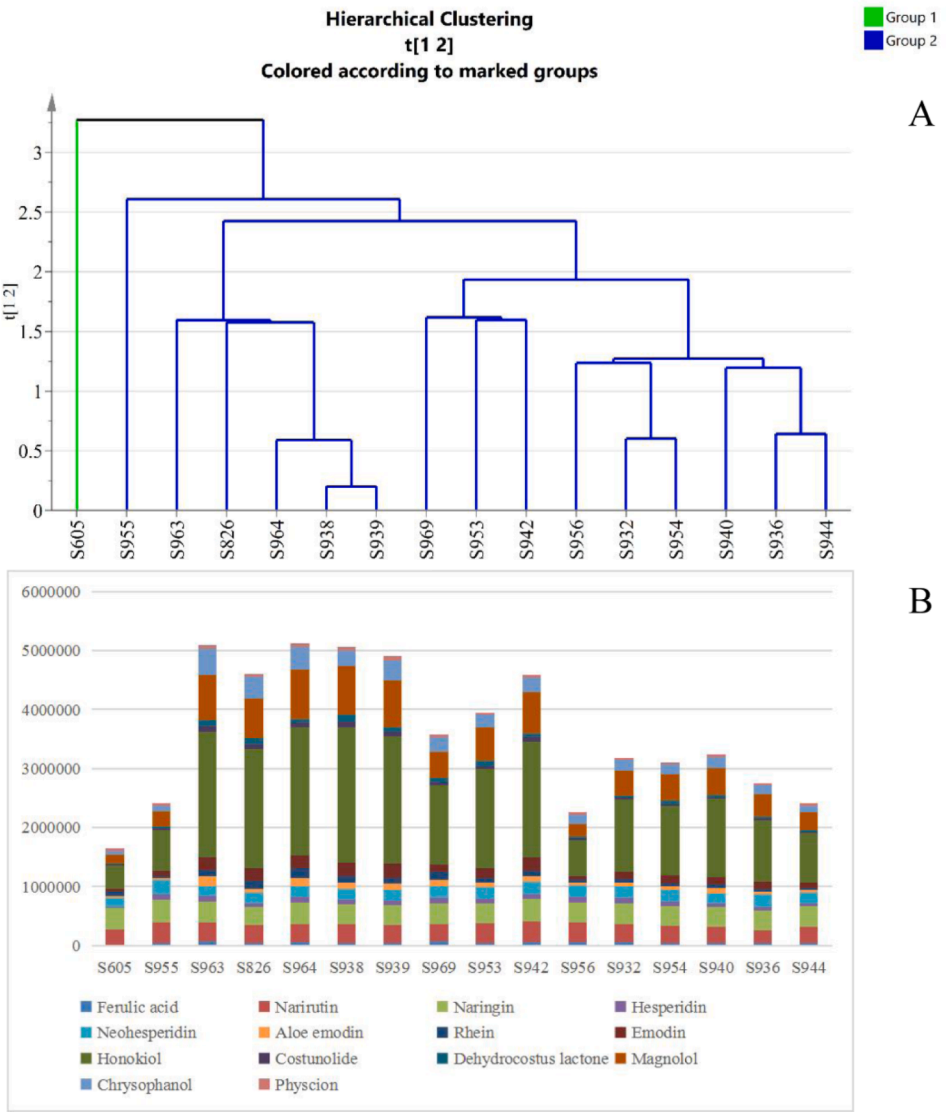

Fig. 3. Hierarchical cluster analysis of WCAP methanol extracts (A), Bar chart of the sum of peak areas in 16 batches of WCAP (B).

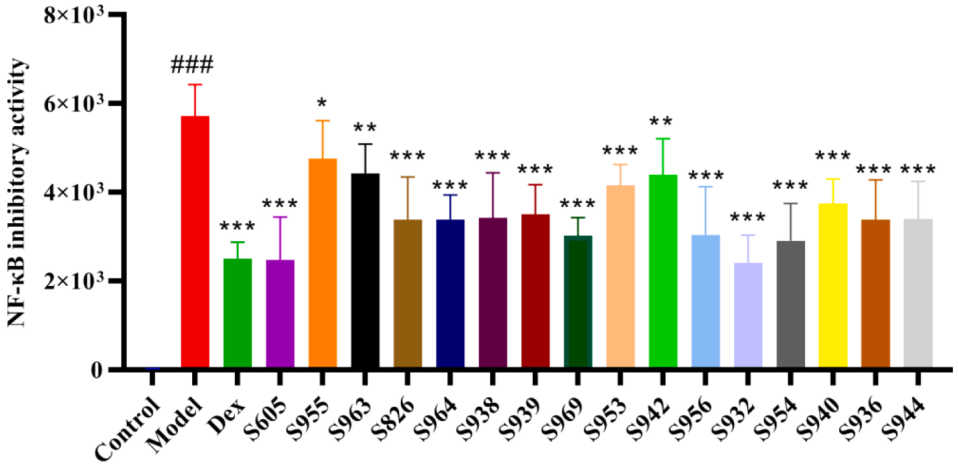

Fig. 4. NF-κB inhibitory activity of 16 batches WCAP methanol extracts ### $p < 0.001$ VS Control, * $p < 0.05$ VS Model, ** $p < 0.01$ VS Model, *** $p < 0.001$ VS Model.

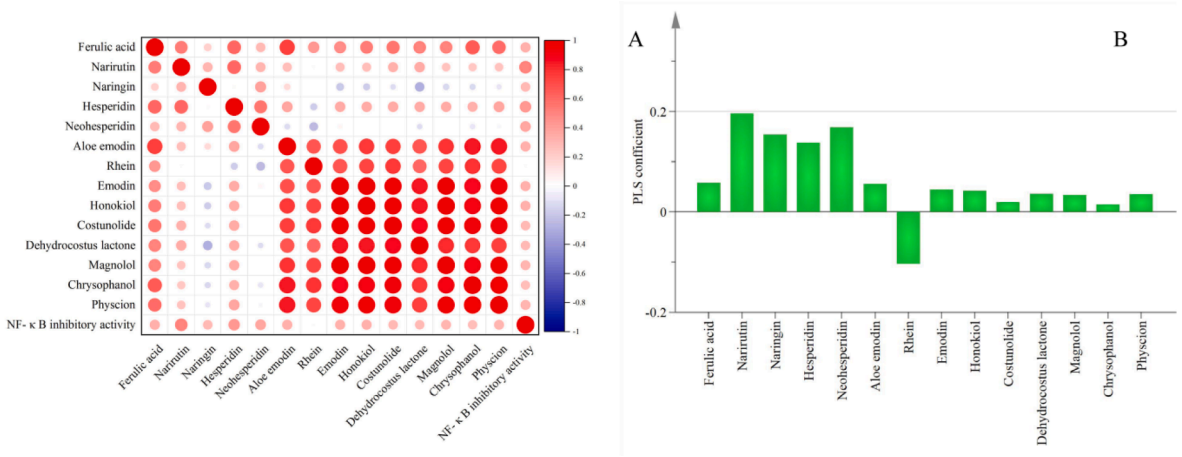

Fig. 5. Pearson correlation results between potential quality markers in all WCAP methanol extracts (A), PLS variation coefficients of 14 chromatographic peaks with NF-κB inhibitory activity (B).

Table 4
The Pearson correlation coefficients between potential quality markers in all WCAP methanol extracts.

compound	Pearson correlation coefficient	compound	Pearson correlation coefficient
Ferulic acid	0.33	Emodin	0.33
Narirutin	0.51	Honokiol	0.33
Naringin	0.34	Costunolide	0.29
Hesperidin	0.43	Dehydrocostus lactone Dehydrocostus lactone	0.29
Neohesperidin	0.37	Magnolol	0.32
Aloe emodin	0.34	Chrysophanol	0.28
Rhein	−0.01	Physcion	0.31

3.8. Determination of the main chemical composition of WCAP

A rapid and efficient UPLC-DAD method was developed to determine the content of the 13 components of WCAP was determined, the precision, repeatability, stability, and recoveries (Table S5) met the requirements. The content of three batches of WCAP was determined by this method and the contents of naringenin and naringin were more than 4.3 mg/g, magnolol and honokiol were more than 3.0 mg/g, and the total amount of anthraquinones in rhubarb was more than 1.05 mg/g. The specific values are presented in supporting material Table S8. The chromatogram of S939 is shown in Fig. 7. The proposed method can be applied as a potent tool for the quality control of WCAP. The content overlay map of 13 quantitative components is shown in Fig S1, and the results are basically consistent with the peak area overlay map in 3.3, which can be mutually supported by the clustering analysis results.

4. Conclusion and discussion

We identified 129 chemical components from WCAP and the Phthalides derived from Chuanxiong were identified for the first time. 10 compounds are likely to be active components to exert NF-κB inhibitory activity by a spectral activity relationship analysis. A quantitative analysis method was established and indicator component of the Adjuvant medicine Chuanxiong was added. In summary, the comprehensive method combining spectral effect and quantification could provide data support for screening the effect substance basis and the selection of quality control index components for WCAP.

Qualitative analysis was conducted on the methanol extract of WCAP using methods such as UHPLC-QE-MS. A total of 129 chemical components were identified in Table 1, mainly from *Aurantii Fructus*, *Rhei Radix et Rhizoma*, *Magnoliae Officinalis Cortex*, *Aucklandiae Radix*, *Chuanxiong Rhizoma* and *Aquilariae Lignum Resinatum*. However, the identification of components in medicinal materials such as *Crotonis Semen Pulveratum*, *Santali Albi Lignum*, and *Moschus* was relatively rare or not identified, possibly because the higher content of components in them were all volatile components, the components with higher content in *Jujubae*

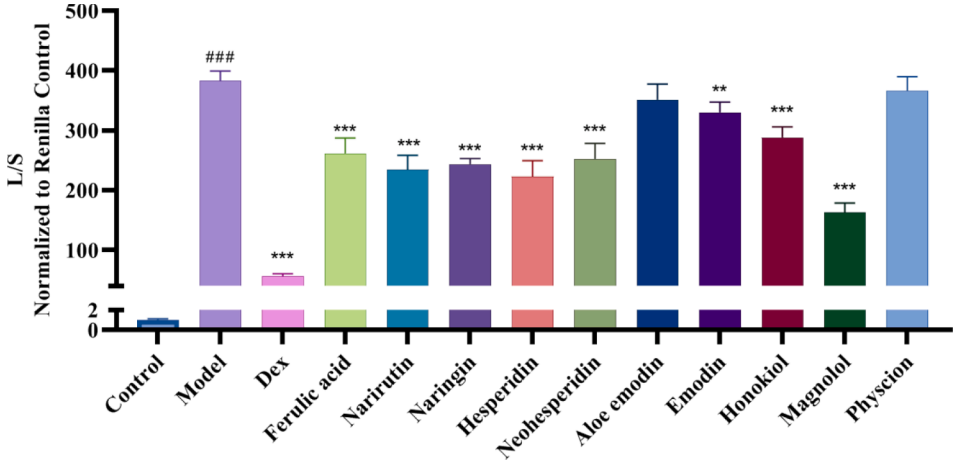

Fig. 6. NF-κB inhibitory activity of the 10 compounds in WCAP ### $p < 0.001$ VS Control, ** $p < 0.01$ VS Model, *** $p < 0.001$ VS Model.

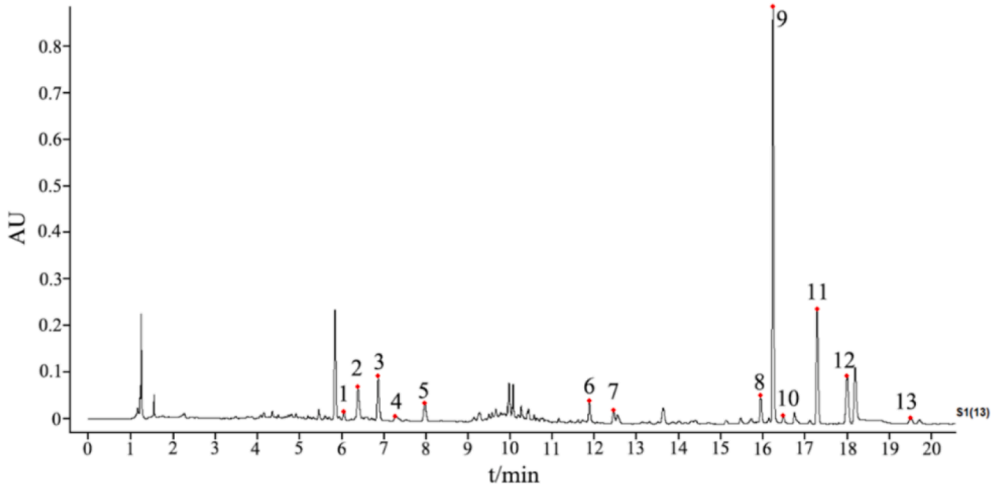

Fig. 7. The UPLC chromatogram of WCAP in 254 nm (1. Ferulic acid; 2. Narirutin; 3. Naringin; 4. Hesperidin; 5. Neohesperidin; 6. Aloe emodin; 7. Rhein; 8. Emodin; 9. Honokiol; 10. Costunolide; 11. Magnolol; 12. Chrysophanol; 13. Physcion.).

Fructu sinclude polysaccharides, proteins, and amino acids, which may be due to the unsuitable chromatographic column and mass spectrometry conditions for detecting such components.

The four compounds of rhein, costunolide, dehydrocostus lactone, and chrysophanol were not screened out. At present, it indeed reported that these four compounds alone have NF- κB inhibitory activity and anti-inflammatory activity when administrated as pure compound. 80 μM rhein showed NF- κB inhibition on LPS-induced RAW264.0 cells (Wen et al., 2020), the three compounds of chrysophanol, costunolide, and dehydrocostus lactone have anti-inflammatory activity (Song et al., 2019; He et al., 2019; Yuan et al., 2022). NF-κB plays a crucial role in the main pharmacological effect of WCAP, these four components may contribute less to the NF- κB inhibitory activity in the complicated WCAP, so it was not screened out through the spectral efficiency relationship method. Therefore, these four compounds may not be components of concern for quality control of WCAP.

In the chemometrics research, we found that the cluster analysis results were consistent with the sum of the peak areas. Components including magnolol, honokiol, naringin, narirutin, and neohesperidin accounted for a large proportion in the sum of the peak areas, and thus play a main role in batch classification. In both the cluster analysis and the fingerprint similarity evaluation, S605 was different from the other batches (the similarity is 0.856). S605 was manufactured much earlier than other batches, and the storage time may have an impact on the chemical composition content. The differences in chemical composition may also be caused by the raw herbal material, reminding the importance of fixed medicinal materials and harvesting conditions in the production of TCM.

10 compounds are likely to exert NF-κB inhibitory activity by combining analysis of the Pearson correlation analysis and PLSR. The four active components with regression coefficients greater than 0.1 were narirutin, naringin, hesperidin, and neohesperidin. The first three compounds have been reported to have NF-κB inhibitory activity (Wang et al., 2020; Zhao et al., 2016; Ha et al., 2012). Neohesperidin has a protective effect on DSS induced colitis (Liu et al., 2022), and this paper reports the NF-κB inhibitory activity of neohesperidin for the first time. The present work demonstrated that the spectrum-effect relationship analysis can quickly find the effect components from complex TCM extracts for the screening of quality control biomarkers, which could be considered as a reference to establish the quality control method for other Chinese patent medicines.

Declaration of Competing Interest

The authors declare that they have no known competing financial interests or personal relationships that could have appeared to influence the work reported in this paper.

Acknowledgements

This study was supported by the Tianjin Committee of Science and Technology of China (22ZYJDSS00040 and 21ZYJDJC00080), Science and Technology Project of Haihe Laboratory of Modern Chinese Medicine(22HHZYSS00007).

Appendix A. Supplementary material

Supplementary data to this article can be found online at https://doi.org/10.1016/j.arabjc.2023.105328.

References

An, Q., Wang, L., Ding, X.Y., et al., 2022. Validation of Sennae Folium specification grade classification based on UPLC-Q-TOF/MS spectrum-effect relationship. Arab. J. Chem. 15 (11).

Chen, H.C., Fu, W.Y., Chen, H.Y., et al., 2019. Magnolol attenuates the inflammation and enhances phagocytosis through the activation of MAPK, NF-κB signal pathways in *vitro* and in *vivo*. Mol. Immunol. 105, 96–106. https://doi.org/10.1016/j.molimm.2018.11.008.

Chen, D., Li, H.T., Xie, G.Y., et al., 2020. Spectrum-effect relationship analysis for antioxidant of Bletilla striata (Thunb.) Reichb. f. based on sparse partial least squares regression. Chin. Wild Plant Resour. 39 (11), 1–6.

Chen, Y.E., Xu, S.J., et al., 2021. Asperuloside suppressing oxidative stress and inflammation in DSS-induced chronic colitis and RAW 264.7 macrophages via Nrf2/HO-1 and NF-κB pathways. Chem. Biol. Interact. 344, 109512 https://doi.org/10.1016/j.cbi.2021.109512.

Chen, Y.L., Zheng, H., Zhang, J.Z., et al., 2016. Protective effect and potential mechanisms of Wei Chang An pill on high-dose 5-fluorouracil-induced intestinal mucositis in mice. J. Ethnopharmacol. 190, 200–211. https://doi.org/10.1016/j.jep.2016.05.057.

Commission, C. P., 2020. Pharmacopoeia of the People's Republic of China. Volume I. Beijing, China Med. Sci. Press.

Gordon, J.W., Shaw, J.A., Kirshenbaum, L.A., 2011. Multiple facets of NF-κB in the heart: to be or not to NF-κB. Circ. Res. 108 (9), 1122–1132. https://doi.org/10.1161/CIRC.

Ha, S.K., Park, H.Y., Eom, H., et al., 2012. Narirutin fraction from citrus peels attenuates LPS-stimulated inflammatory response through inhibition of NF-κB and MAPKs activation. Food Chem. Toxicol. 50 (10), 3498–3504. https://doi.org/10.1016/j.fct.2012.07.007.

Han, M.C., Xie, R.N., Yang, M.Q., et al., 2021. Research method of spectrum-effect relationship and its application in traditional Chinese medicine research. Guangzhou Chem. Ind. 49 (10), 16–19.

Han, Y., Zhou, M., Wang, L., et al., 2015. Comparative evaluation of different cultivars of Flos Chrysanthemi by an anti-inflammatory-based NF-κB reporter gene assay

coupled to UPLC-Q/TOF MS with PCA and ANN. J. Ethnopharmacol. 174, 387–395. https://doi.org/10.1016/j.jep.2015.08.044.
He, Y., Moqbel, S.A.A., Xu, L., et al., 2019. Costunolide inhibits matrix metalloproteinases expression and osteoarthritis via the NF-κB and Wnt/β-catenin signaling pathways. Mol. Med. Rep. 20 (1), 312–322. https://doi.org/10.3892/mmr.2019.10239.
Jing, Y.K., Song, X., Chai, X., et al., 2012. Quantitation and qualitation of eleven components in Wei Chang An pill by ultra-performance liquid chromatography-UV-tandem mass spectrometry. J. Pharm. Anal. 32 (07), 1165–1170.
Kunnumakkara, A.B., Shabnam, B., Girisa, S., et al., 2020. Inflammation, NF-κB, and Chronic Diseases: how are they linked ? Crit. Rev. Immunol. 40 (1), 1–39. https://doi.org/10.1615/CritRevImmunol.2020033210.
Liu, Z.M., Li, L.L., Huang, Y.F., et al., 2022. Protective effect and mechanism of neohesperidin in mice with DSS-induced ulcerative colitis. Mod. Prev. Med. 49 (24), 4505–4512. https://doi.org/10.20043/j.cnki.MPM.202204578.
Liu, Z., Zhang, J., Gao, W., et al., 2013. Antinociceptive activity and chemical composition of Wei Chang An pill extracts. Pharm. Biol. 51 (6) https://doi.org/10.3109/13880209.2013.766893.
Makó, V., Czúcz, J., Weiszhár, Z., et al., 2010. Proinflammatory activation pattern of human umbilical vein endothelial cells induced by IL-1β, TNF-α, and LPS. Cytometry A 77 (10), 962–970. https://doi.org/10.1002/cyto.a.20952.
Shang, W.G., Xu, H., 2020. Clinical effect of Wei Chang An pill in the treatment of child patients with rotavirus enteritis and its influence on myocardial enzyme spectrum. China J. Pharm. Econ. 15 (11), 74–77.
Shi, F., Hao, X.M., Liu, Y., et al., 2018. Clinical effect evaluation of Wei Chang An pill in treating functional diarrhea. Clin. J. Chin. Med. 10 (33), 14–18.
Song, G., Zhang, Y., Yu, S., et al., 2019. Chrysophanol attenuates airway inflammation and remodeling through nuclear factor-kappa B signaling pathway in asthma. Phytother. Res. 33 (10), 2702–2713. https://doi.org/10.1002/ptr.6444.
Tse, A.K., Wan, C.K., Shen, X.L., et al., 2005. Honokiol inhibits TNF-alpha-stimulated NF-kappaB activation and NF-κB-regulated gene expression through suppression of IKK activation. Biochem. Pharmacol. 70 (10), 1443–1457. https://doi.org/10.1016/j.bcp.2005.08.011.
Wang, S., He, N., Xing, H., et al., 2020. Function of hesperidin alleviating inflammation and oxidative stress responses in COPD mice might be related to SIRT1/PGC-1α/NF-κB signaling axis. J. Recep. Signal Transduct. Res. 40 (4), 388–394. https://doi.org/10.1080/10799893.2020.1738483.
Wang, L.J., Jiang, Z.M., Xiao, P.T., et al., 2019. Identification of anti-inflammatory components in Sinomenii Caulis based on spectrum-effect relationship and chemometric methods. J. Pharm. Biomed. Anal. 167, 38–48. https://doi.org/10.1016/j.jpba.2019.01.047.
Wen, Q., Miao, J., Lau, N., et al., 2020. Rhein attenuates lipopolysaccharide-primed inflammation through NF-κB inhibition in RAW264.7 cells: targeting the PPAR-γ signal pathway. Can. J. Physiol. Pharmacol. 98 (6), 357–365. https://doi.org/10.1139/cjpp-2019-0389.
Xu, J., Li, S.X., Yang, X.F., et al., 2022. Mechanism of nonylphenol induced gastric inflammation through NF-κB/NLRP3 signaling pathway. Toxicology 479, 153294. https://doi.org/10.1016/j.tox.2022.153294.
Yu, H., Lin, L., Zhang, Z., et al., 2020. Targeting NF-κB pathway for the therapy of diseases: mechanism and clinical study. Signal Transduct. Target. Ther. 5 (1), 209. https://doi.org/10.1038/s41392-020-00312-6.
Yuan, Y., Hu, Q., Liu, L., et al., 2022. Dehydrocostus lactone suppresses dextran sulfate sodium-induced colitis by targeting the IKKα/β-NF-κB and Keap1-Nrf2 signalling pathways. Front. Pharmacol. 13, 817596 https://doi.org/10.3389/fphar.2022.817596.
Zhang, J.Z., Gao, W.Y., Ma, C.Y., et al., 2010. Analysis on chemical components in Wei Chang An pill. Drug Eval. Res. 33 (02), 116–120.
Zhang, J.Z., Gao, W.Y., Liu, Z., et al., 2013. Identification and simultaneous determination of twelve active components in the methanol extract of traditional medicine Wei Chang An pill by HPLC-DAD-ESI-MS/MS. Iran. J. Pharm. Res. 12 (1), 15–24.
Zhang, T., Su, X.L., Mao, X.Y., et al., 2020. Effects of Wei Chang An pill on Treg/Th17 immune balance in ulcerative colitis model mice. J. Tradit. Chin. Med. 61 (22), 1983–1989.
Zhao, Y., Li, Z., Wang, W., et al., 2016. Naringin protects against cartilage destruction in osteoarthritis through repression of NF-κB signaling pathway. Inflammation. 39 (1), 385–392. https://doi.org/10.1007/s10753-015-0260-8.
Zhu, C.S., Lin, Z.J., Xiao, M.L., et al., 2016. The spectrum-effect relationship-a rational approach to screening effective compounds, reflecting the internal quality of Chinese herbal medicine. Chin. J. Nat. Med. 14 (3), 177–184. https://doi.org/10.1016/S1875-5364(16)30014-0.